CENTRO DE TECNOLOGÍAS DE LA IMAGEN

CTIM Technical Report

ISSN 2254-2353

Implementation of a Robust Optical Flow Method for Color Images

Nelson Monzón López, Javier Sánchez Pérez and Agustín J. Salgado de la Nuez

No. 4

Las Palmas de Gran Canaria
03 September 2014

Implementation of a Robust Optical Flow Method for Color Images

Nelson Monzón, Javier Sánchez and Agustín Salgado
Centro de Tecnologías de la Imagen
Universidad de Las Palmas de Gran Canaria
35017 Las Palmas de Gran Canaria, Spain

Abstract

We analyse the influence of colour information in optical flow methods. Typically, most of these techniques compute their solutions using grayscale intensities due to its simplicity and faster processing, ignoring the colour features. However, the current processing systems have minimized their computational cost and, on the other hand, it is reasonable to assume that a colour image offers more details from the scene which should facilitate finding better flow fields. The aim of this work is to determine if a multi-channel approach supposes a quite enough improvement to justify its use. In order to address this evaluation, we use a multi-channel implementation of a well-known TV-L^1 method. Furthermore, we review the state-of-the-art in colour optical flow methods. In the experiments, we study various solutions using grayscale and RGB images from recent evaluation datasets to verify the colour benefits in motion estimation.

Keywords: Optical Flow, Motion Estimation, Variational Techniques, Image Registration.

1 Introduction

Optical flow estimation is a key problem in computer vision that serves as a low-level basis for motion recovery. It can be used as an initial stage for many high-level applications, such as robot guiding, motion coordination of UAVs, objects tracking, obstacles detection, time to collision, 3D scene reconstruction and others. Owing to its importance and multiple uses, it has received much attention during the last three decades.

In the literature, the variational methods have been the most widely used techniques due to its robustness and accuracy. Typically, these approximations obtain their solutions as a minimization of an energy functional. This energy is a weighted sum of a data term that puts into correspondences pixels from consecutive images and a regularizing term that imposes a constraint on the continuity of the flow.

Because of their good results, numerous contributions have been proposed since the classical work of Horn and Schunck [13] like, for instance, different smoothing strategies [18, 2, 26] to cope with motion discontinuities, robust penalization [9, 28], temporal coherence [8, 20, 21] and many others.

All of these approaches share the same premise in the data term, which is commonly known as the *brightness constancy assumption*. It consists in associating the motion field with brightness changes in the image, assuming that the intensity remains constant through the sequence. In this sense, the luminance information is crucial to achieve good solutions, especially when dealing with strong lighting variations.

Despite this evidence, the optical flow problem is usually solved by using grayscale intensities ignoring the multi-channel information of colour images. In fact, it is common to convert the original colour image into grayscale in order to decrease the algorithm complexity and lower execution times.

Nevertheless, using a single channel of information has one decisive drawback due to the fact that the grayscale values are susceptible to slight changes in brightness, which often appear in real scenes. A colour image could prevent this situation by associating the pixel information with various brightness intensities. Even, the colour information may avoid the use of additional constraints in the flow calculation [12, 19] and contains more photometric information that can be useful against shadows, shading and image specularities [6, 24, 16].

A colour image is a representation of a scene built as a combination of different features stored by multiple channels of information. Depending of their characteristics and the number of channels we can find various image models. Probably, the most commonly known is the RGB, that uses three channels for matching red, green and blue light components to reproduce a broad array of colours. A grayscale image is quite similar to this model but using a single channel of luminance information.

The HSV and YUV models are cylindrical-coordinate representations that store image information in three channels. In both cases, the information is decomposed in one channel for the brightness and two for the chrominance. The difference resides in the colour representation: while the HSV model describes it as a vector in polar form, the YUV system uses an orthogonal three dimensional space of the colour plane. The three channel UCS colour model gives an uniform chromaticity space based on measurements of human colour perception. This measure is denoted by the Euclidean distance that corresponds linearly to the colour perception or changes in the intensity.

We can also find other alternatives like, for instance, the CMYK model that composes the scene by mixing four channels of information (cyan, magenta, yellow and black) or satellite images. This last model can be defined as a visual representation captured by multiple electromagnetic spectrum channels of a sensor mounted on an artificial satellite.

Given this broad variety of images, the use of colour in variational techniques may be interesting for calculating the flow. In this sense, Barron and Klette [6] introduced the classical work of Horn and Schunck in a multi-channel framework. Following this idea, Mileva *et al.* [16] modified the original model of Brox *et al.* [9] into a multi-channel approach to investigate the flow behaviour under realistic illumination conditions.

The latter work uses a TV-L^1 scheme in the smoothness term that provides piecewise continuous flows. It also deals with brightness changes by including a gradient constancy assumption in its energy functional in conjunction with the brightness constancy assumption.

Later, Sánchez *et al.* [23] conducted a thorough analysis of this variational model using its own implementation. This work exposed the major drawbacks of the method, especially the appearance of rounding shapes at the flow edges. Monzón *et al.* [17] introduced a discontinuity preserving strategy to avoid this problem based on the idea proposed in [25, 27]. In relation to this, a multi-channel framework could ameliorate this situation by including colour information.

Although this proposal has been improved since its publication, it still provides highly accurate optical flow fields and is a reference in variational techniques. Thus, we have developed a multi-channel extension of the implementation presented in Sánchez *et al.* [23] for our experiments.

Then, the aim of our research work is twofold: first, we present a study of different proposals in colour optical flow; second, we use this multi-channel technique to determine if the colour information benefits the optical flow calculation.

We perform our evaluation with the widely used sequences from the Middlebury benchmark database [4] and the open source movies from the MPI-Sintel flow data set [10]. Our experiments demonstrate that, in general, the colour information provides more accurate solutions and the computational cost seems reasonable given the improvement.

Our work is organized as follows: first, we present a survey of colour optical flow methods in Section 2; second, in Section 3 we introduce the general framework behind the multi-channel method; then, we analyse the behaviour of colour and grayscale information in the experimental results of Section 4; next, we study the accuracy and the performance of both colour spaces in Section 5; finally, a summary of the main ideas and conclusions in Section 6.

2 Related Work

During the last years, various works have focused their efforts in analysing and proposing the use of colour information in optical flow methods. In 1989, Ohta [19] proposed a method to obtain the optical flow directly from an image pixel without imposing any other assumption [11, 13]. Thus, his approach derived multiple conditions from the multi-channel information of a single image point. Later, Markandey and Flinchbaugh [15] presented a numerical scheme that uses the visible and the infra-red spectrum from a multispectral image.

In 1997, Golland and Bruckstein [12] analysed the robustness of colour models by presenting two methods for motion estimation. The first one assumes brightness conservation under motion considering a multi-channel image as a set of three different grayscale images. The second introduced the idea of *colour conservation* under the premise that its components (not only the luminance) are conserved. Their experiments confirmed that, in regions with strong gradient, good solutions can be obtained, whereas in regions of uniform chrominance these methods failed. This work used RGB, normalized RGB and HSV images to evaluate their proposals.

Later, Barron and Klette [5] examined the previous approaches [19, 12] and multi-channel extensions of the models of Lucas and Kanade [14] and Horn and Schunck [13]. Their comparison concluded that the colour presents advantages in optical flow computation. Besides, they observed that its use does not increase excessively the execution time. In [6], these authors reasserted their conclusions but determining, additionally, that the saturation channel worsen the motion fields.

Andrews and Lowell [3] compared the previous results of [14, 13] with YUV and UCS colour spaces. They also developed new implementations of [12, 6] with the aim of decreasing their computational costs.

In 2004, the state-of-the-art of colour optical flow intensified its efforts to achieve robust motion fields, even under severe luminance conditions and noisy images, from the photometric information that the colour provides. With this objective, Weijer and Grevers [24] proposed a method based on the dichromatic reflection model of Schafer [22] for deriving photometric invariances against shadows, shading and specularities. Furthermore, their model incorporated a reliability measure for dealing with the instabilities that appear on the flow because of the photometric invariants.

Based on this premise, Mileva *et al.* [16] proved in their experiments that a variational method improves its solutions against realistic illumination conditions by replacing the classical brightness assumption with photometric invariants. A few years later, Zimmer *et al.* [28] proposed a robust data term against outliers and variable luminance. Among other features, it uses the HSV colour space with separate robustification for each channel. This idea is interesting because the HSV representation offers distinct levels of photometric invariance, so we can use the most confident channel in our estimation. In 2010, Bin *et al* [7] presented an approach that computes their solutions by extending the typical optical flow constraints. Their intention was to deal with movements like rotations, deformation objects motion and light variations.

Álvarez *et al.* [1] contributed in the use of multi-channel images in optical flow. This work studied how to combine different channels of satellite images like, infra-red or intensity, to follow the evolution of the clouds.

3 Multi-Channel Optical Flow

Let $\mathbf{I}(\mathbf{x}) : \Omega \subset \mathbb{R}^3 \rightarrow \mathbb{R}^C$ be an image sequence, with $\mathbf{x} = (x, y, t)^T \in \Omega$, $\mathbf{I} = \{I^c\}_{c=1,\dots,C}$ and C the number of channels. We define the optical flow as a dense mapping, $\mathbf{w}(\mathbf{x}) = (u(\mathbf{x}), v(\mathbf{x}), 1)^T$, between every two consecutive images, where $u(\mathbf{x})$ and $v(\mathbf{x})$ are the vector fields that represent the x and y displacements, respectively. We use $\nabla\mathbf{I} = \{(I_x^c, I_y^c)^T\}_{c=1,\dots,C}$ to denote the spatial gradient of the image, with I_x^c, I_y^c the first order derivatives in x and y for each information channel.

Following the original model [9, 23], we assume that the brightness constancy assumption is also fulfilled in the multi-channel scheme. Then, according to this notation, our energy functional reads as:

$$
\begin{aligned}
E(\mathbf{w}) = &\int_\Omega \Psi\left(\|\mathbf{I}(\mathbf{x}+\mathbf{w}) - \mathbf{I}(\mathbf{x})\|^2\right) \mathbf{dx} \\
&+ \gamma \int_\Omega \Psi\left(trace\left(\left(\nabla\mathbf{I}(\mathbf{x}+\mathbf{w}) - \nabla\mathbf{I}(\mathbf{x})\right)\left(\nabla\mathbf{I}(\mathbf{x}+\mathbf{w}) - \nabla\mathbf{I}(\mathbf{x})\right)^T\right)\right) \mathbf{dx} \\
&+ \alpha \int_\Omega \Psi\left(\|\nabla u(\mathbf{x})\|^2 + \|\nabla v(\mathbf{x})\|^2\right) \mathbf{dx}, \qquad (1)
\end{aligned}
$$

with $\Psi\left(s^2\right) = \sqrt{s^2 + \epsilon^2}$ as a robustification function and ϵ as a prefixed small constant to ensure that Ψ is strictly convex. We use the Euclidean norm, $\|\mathbf{v}\| = \sqrt{\sum_{i=1}^N v_i^2}$.

The energy model of Brox *et al.* uses brightness and gradient constancy assumptions in the data term and a TV scheme for smoothing. It depends on the γ and α parameters for controlling the gradient and the smoothness strength, respectively.

The solution is obtained by minimizing the energy functional (1). This minimum can be found by solving the following Euler-Lagrange equations, that are quite similar to the original proposal:

$$
\begin{aligned}
0 = &\Psi'_D \cdot \left(\sum_{c=1}^{C} \left(I^c(\mathbf{x}+\mathbf{w}) - I^c(\mathbf{x})\right) \cdot I_x^c(\mathbf{x}+\mathbf{w})\right) \\
&+ \gamma\, \Psi'_G \cdot \left(\sum_{c=1}^{C} \left(I_x^c(\mathbf{x}+\mathbf{w}) - I_x^c(\mathbf{x})\right) \cdot I_{xx}^c(\mathbf{x}+\mathbf{w}) + \left(I_y^c(\mathbf{x}+\mathbf{w}) - I_y^c(\mathbf{x})\right) \cdot I_{xy}^c(\mathbf{x}+\mathbf{w})\right) \\
&- \alpha\, \mathrm{div}\left(\Psi'_S \cdot \nabla u\right), \\
0 = &\Psi'_D \cdot \left(\sum_{c=1}^{C} \left(I^c(\mathbf{x}+\mathbf{w}) - I^c(\mathbf{x})\right) \cdot I_y^c(\mathbf{x}+\mathbf{w})\right) \\
&+ \gamma\, \Psi'_G \cdot \left(\sum_{c=1}^{C} \left(I_x^c(\mathbf{x}+\mathbf{w}) - I_x^c(\mathbf{x})\right) \cdot I_{xy}^c(\mathbf{x}+\mathbf{w}) + \left(I_y^c(\mathbf{x}+\mathbf{w}) - I_y^c(\mathbf{x})\right) \cdot I_{yy}^c(\mathbf{x}+\mathbf{w})\right) \\
&- \alpha\, \mathrm{div}(\Psi'_S \cdot \nabla v), \qquad (2)
\end{aligned}
$$

with $\Psi'(s^2) = \frac{1}{2\sqrt{s^2+\epsilon^2}}$. Notice that the difference with respect to the original model resides in the summatory of image channels included in both constancy assumptions of the data term. As a consequence, the influence of this term is increased proportional to the number of channels. We compensate this situation by adapting the smoothness parameter α, therefore, $\alpha = \alpha' \cdot C$, being α' an input parameter. An example of this multi-channel scheme can be seen in Fig. 1. We use the following abbreviations:

$$\begin{aligned}
\Psi'_D :=& \Psi'\left(\|\mathbf{I}(\mathbf{x}+\mathbf{w})-\mathbf{I}(\mathbf{x})\|^2\right)\\
\Psi'_G :=& \Psi'\left(trace\left(\left(\nabla\mathbf{I}(\mathbf{x}+\mathbf{w})-\nabla\mathbf{I}(\mathbf{x})\right)\left(\nabla\mathbf{I}(\mathbf{x}+\mathbf{w})-\nabla\mathbf{I}(\mathbf{x})\right)^T\right)\right)\\
\Psi'_S :=& \Psi'\left(\|\nabla u\|^2+\|\nabla v\|^2\right).
\end{aligned} \tag{3}$$

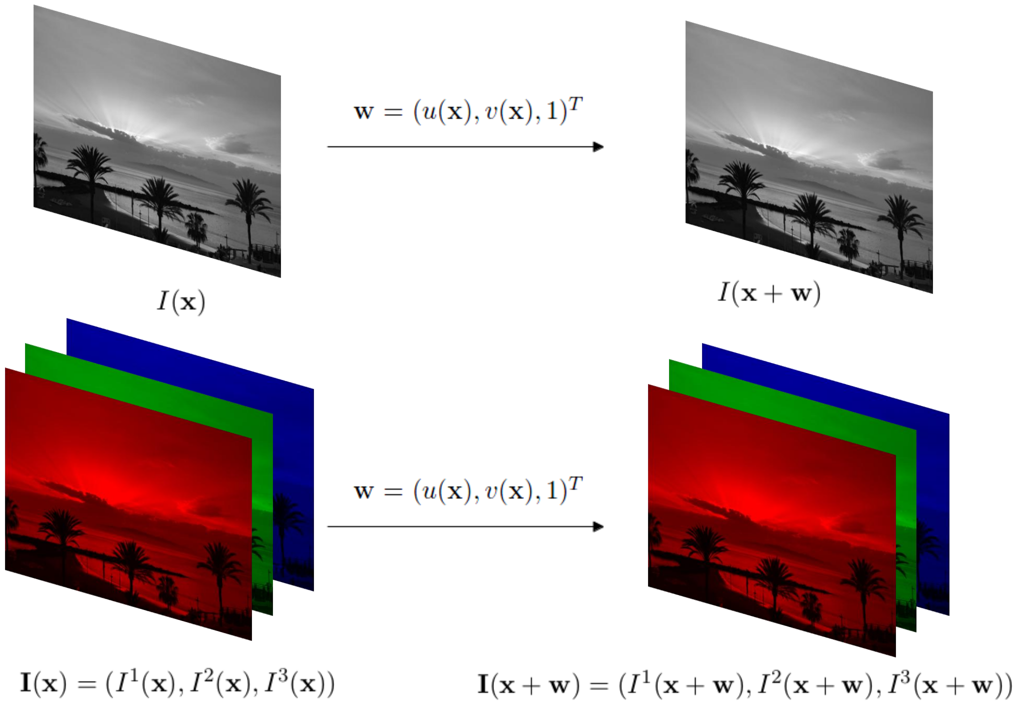

Figure 1: Notation for grayscale and colour images.

We use centered finite differences to discretize the system. Then, the system of equations (2) is solved by means of an iterative approximation, such as the SOR method. On the other hand, the above formulas (3) are nonlinear because of $\mathbf{w}$ and Ψ'; so, in order to linearise the equations, the numerical scheme is enclosed in two fixed point iterations. We also embedded it in a multiscale strategy to allow detecting large displacements. Starting from the coarsest scale, we obtain a solution that will be progressively refined in the finer scales. Besides, we use *motion increments*, $\mathbf{w}^{k+1} = \mathbf{w}^k + \mathbf{dw}^k$, so $\mathbf{dw}^k$ can be iteratively estimated in each scale until finding the final optical flow. The warping of $\mathbf{I}(\mathbf{x}+\mathbf{w})$ is approximated using Taylor series and bicubic interpolation. More details about the implementation of this scheme are given in [9] or, more extensively, in [23].

4 Experimental Results

In this section, we present an evaluation of the possible benefits of colour against grayscale information in a variational optical flow method. We show the experiments for some synthetic sequences from the Middlebury benchmark database and MPI-Sintel dataset using RGB and grayscale images. The purpose of these tests is to compare motion details between the best flows achieved for the same sequence. We have made our evaluation using the best configuration of α and γ for every sequence. The remaining parameters are set as in [23].

Figures 2, 3 and 4 show the results for the Middlebury sequences of *Grove3*, *RubberWhale* and *Urban2*, respectively. On the other hand, Figures 5, 6 and 7 depict the best flows and its details for the sequences of *Bandage 1*, *Bandage 2* and *Ambush 5* from MPI-Sintel dataset.

In the first column of these figures, we show the colour scheme used for the optical flow representation, the grayscale and the colour images. In the second column, we depict the ground truth and the motion fields for grayscale and RGB, respectively. The remaining columns present motion details for the corresponding solutions. The colour scheme represents the orientation and magnitude of the vector field.

According to the results, we conclude that the colour information benefits the optical flow estimation. In general, the motion boundaries are better preserved and the error decreases perceptibly, especially in Figures 2 and 7.

Figure 2 is a good example of this improvement. We can observe that the flow field obtained from the colour image is closer to the ground truth than the grayscale picture. In the detail boxes of the third column, we see that some leafs are better preserved and, in general, the solution is more realistic. The reason of this enhancement is due to the fact that the difference between the leafs and the background is much pronounced in the colour image. The grayscale picture complicates that the method can distinguish the moving objects with respect to the background. Similarly, we observe a more precise contour definition in Figures 3 and 4. In the red box of the colour solution of *RubberWhale* we observe an improvement in a shading region because of the multi-channel information. Nevertheless, the benefits are not so clear in both figures as the previous one.

Figure 5 shows a more accurate result in its third row. In this case, we can also observe that adding more information in the zone depicted by the green box ameliorates the diffusion in the dragon tail. On the other hand, we can see a significant decrease of the error in the head of the dragon at Figure 6.

Finally, although neither of the motion fields of figure 7 offer good results, we observe fewer outliers in the colour solution.

5 Quantitative Results

Next, we show the numerical results provided by the best configurations of α and γ to compare the accuracy of using colour or grayscale in these two datasets. On the other hand, it is interesting to take into account the running times required by the method to justify if the computational cost its reasonable. The values for the remaining parameters have been fixed as in Sect. 4.

First, we depict in Tables 1 and 2 the Average Angular Error (AAE) and the End Point Error (EPE) results for the best settings using the grayscale and colour sequences. The last two columns of these figures show the percentage of error variation between the colour spaces. Observing the results, we can state that the RGB information improves the numerical errors, especially in the Middlebury sequences where most of the amelioration in the EPE exceeds in 5.50% and the AAE in 4%. Notice that we have not presented the Venus sequence in our experiments. Its ground truth does not seem to be correct and the AAE and the EPE may not be well estimated.

Moreover, the enhancement is not so evident in the *MPI Sintel* sequences. It can be appreciated that, in a few occasions, the colour worsens the EPE. Nevertheless, this deterioration is not excessive and the colour information provides a reasonable improvement in a high percentage of cases, especially in *Ambush 5* and *Sleeping 1*.

On the other hand, the error amelioration is not enough to determine if a multi-channel scheme is justified. Thus, Figures 3 and 4 show the execution times needed for obtaining all the previous results. The size of the sequences from MPI Sintel is 1024×436 while, in the case of Middlebury, the size of the images is variable: *Grove2*, *Grove3*, *Urban2* and *Urban3* are 640×480, while *Hydrangea*, *RubberWhale* and *Dimetrodon* are 584×388.

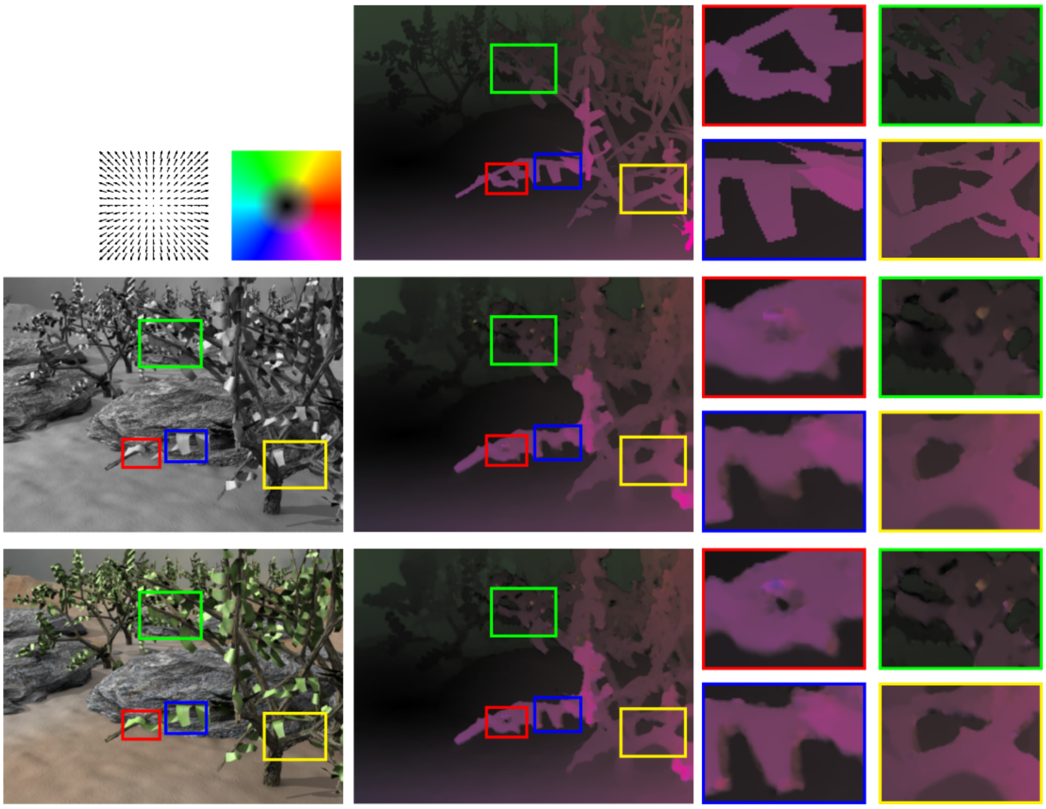

Figure 2: Motion details for the *Grove3* sequence.

Tables 3 and 4 show the runtimes of each sequence and the percentage of improvement provided by the grayscale with respect to the RGB images. As expected, less information means less execution time. However, the difference is not excessively pronounced and, even, in the case of *Ambush 2* sequence, less time is required if we use colour information. This means that, using more information from the images, the algorithm usually converges in less iterations. Moreover, we must consider that the increment in the calculations has only affected the data term, so that more image channels does not mean that the operations grow up proportionally.

The experiments were realized in a computer with the following features: Intel(R) Core(TM) i7 CPU 860 @2.80GHz. We have used a single core in our tests.

Table 1: AAE and EPE for the Middlebury dataset.

	AAE			EPE		
Sequence	**Grayscale**	**RGB**	%	**Grayscale**	**RGB**	%
Grove2	2.198^o	2.169^o	**1.34%**	0.152	0.149	**2.03%**
Grove3	5.971^o	5.661^o	**5.48%**	0.659	0.612	**7.68%**
Hydrangea	2.142^o	2.015^o	**6.30%**	0.180	0.166	**8.43%**
RubberWhale	3.453^o	3.305^o	**4.48%**	0.103	0.097	**6.18%**
Urban2	2.438^o	2.328^o	**4.72%**	0.359	0.340	**5.59%**
Urban3	3.539^o	3.394^o	**4.27%**	0.386	0.401	**-3.74%**
Dimetrodon	1.588^o	1.458^o	**8.91%**	0.083	0.074	**12.16%**

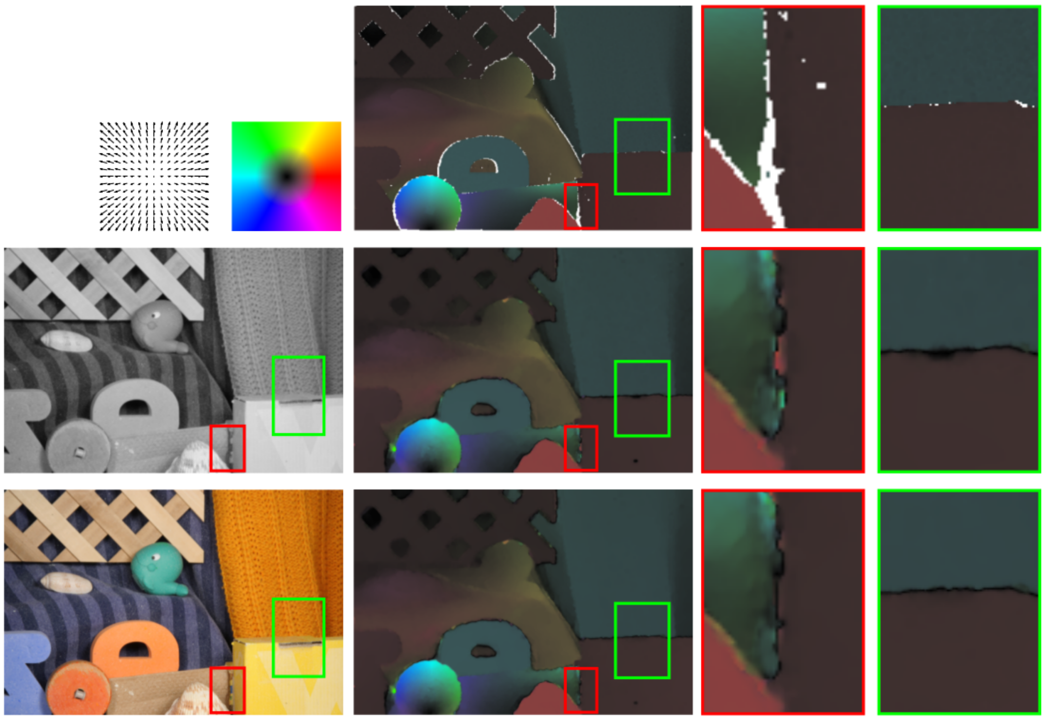

Figure 3: Motion details for the *RubberWhale* sequence.

6 Conclusion

In this work, we studied the influence of colour in variational optical flow methods. We presented a survey in colour proposals for motion estimation and developed a multi-channel implementation of a well-known grayscale method. Our results confirm that: (i) the RGB colour space offers several benefits in motion estimation without using new assumptions in the energy model and (ii) the computational cost does not grow up proportionally to the number of channels.

The multi-channel method decreases the number of outliers and also provides a better preservation of the discontinuities. In general, the colour information allows to increase the accuracy, as we showed in the experiments. However, the improvement in many sequences from the MPI-Sintel database is not so evident. These sequences include many complex effects, such as fog, dust or blur that considerably increase the errors, independently of the image type. In fact, we observe that the colour information ameliorates the solution in regions not affected by these perturbations.

The use of several channels suggests that the algorithm complexity will be higher and the computational cost will augment proportionally. Nevertheless, from the implementation point of view, the modifications introduced in the original model are straightforward. Even more, the runtime does not increase in line with the number of channels due to the following reasons: the changes only affect the data term and, typically, the colour information allows a faster convergence of the algorithm. This cost can also be reduced if we use a multi-core infrastructure.

We may conclude that the benefits of colour information in variational optical flow methods compensate the increment on the execution time.

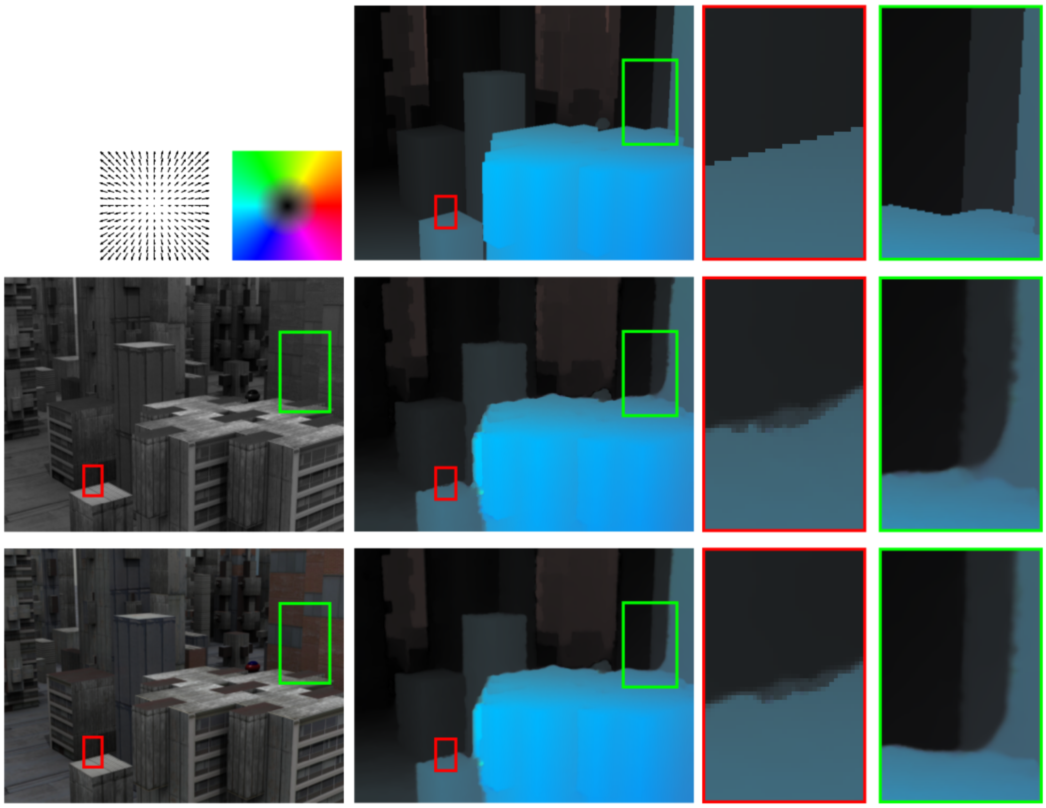

Figure 4: Motion details for the *Urban2* sequence.

Acknowledgements

This work has been partially supported by the Spanish Ministry of Science and Innovation through the research project TIN2011-25488 and University of Las Palmas de Gran Canaria grant ULPGC011-006.

References

[1] L. Álvarez, C.A. Castao, M. Garca, K. Krissian, L. Mazorra, A. Salgado, and J. Snchez. Multi-channel satellite image analysis using a variational approach. *Pure and Applied Geophysics*, 165(6):1071–1093, 2008.

[2] Luis Álvarez, Julio Esclarín, Martin Lefébure, and Javier Sánchez. A pde model for computing the optical flow. In *XVI Congreso de Ecuaciones Diferenciales y Aplicaciones, C.E.D.Y.A. XVI*, pages 1349–1356, Las Palmas de Gran Canaria, Spain, 1999.

[3] Robert J. Andrews and Brian C. Lovell. Color optical flow. In *In Eds. Proceedings Workshop on Digital Image Computing*, pages 135–139, 2003.

[4] Simon Baker, Daniel Scharstein, J. P. Lewis, Stefan Roth, Michael J. Black, and Richard Szeliski. A database and evaluation methodology for optical flow. In *International Conference on Computer Vision*, pages 1–8, 2007. `http://dx.doi.org/10.1109/ICCV.2007.4408903`.

[5] J. Barron and R. Klette. Experience with optical flow in color video image sequences. In *Image and Vision Computing 2001*, pages 195–200, October 2001.

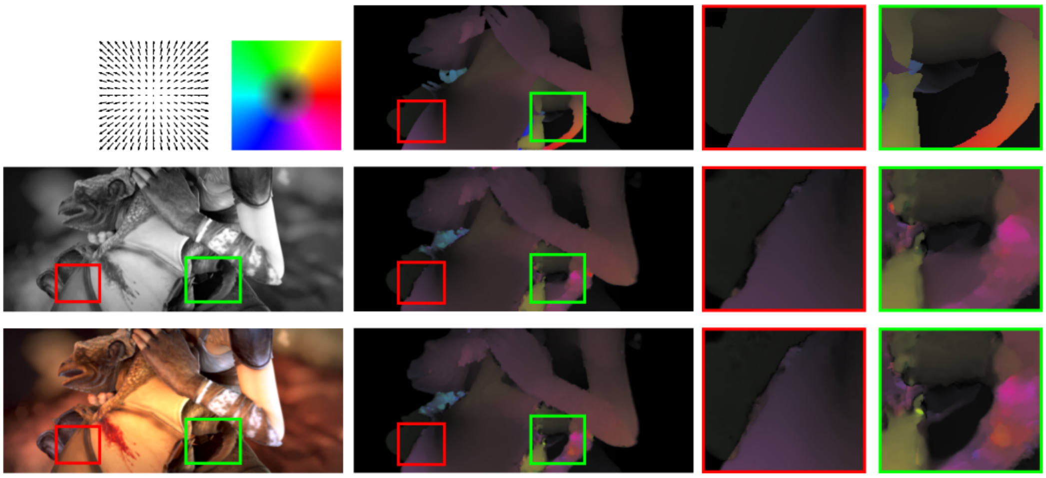

Figure 5: Motion details for the *Bandage 1*.

Figure 6: Motion details for *Bandage 2*.

[6] J. Barron and R. Klette. Quantitative color optical flow. In *Pattern Recognition, 2002. Proceedings. 16th International Conference on*, volume 4, pages 251–255 vol.4, 2002.

[7] Liao Bin, Du Minghui, and Hu Jinlong. Color optical flow estimation based on gradient fields with extended constraints. In *Networking and Information Technology (ICNIT), 2010 International Conference on*, pages 279–283, June 2010.

[8] Michael J. Black and P. Anandan. The robust estimation of multiple motions: Parametric and piecewise-smooth flow fields. *Computer Vision and Image Understanding*, 63(1):75 – 104, 1996.

[9] T. Brox, A. Bruhn, N. Papenberg, and J. Weickert. High accuracy optical flow estimation based on a theory for warping. In T. Pajdla and J. Matas, editors, *European Conference on Computer Vision (ECCV)*, volume 3024 of *LNCS*, pages 25–36, Prague, Czech Republic, May 2004. Springer.

[10] D. J. Butler, J. Wulff, G. B. Stanley, and M. J. Black. A naturalistic open source movie for optical flow evaluation. In A. Fitzgibbon et al. (Eds.), editor, *European Conf. on Computer Vision (ECCV)*, Part IV, LNCS 7577, pages 611–625. Springer-Verlag, October 2012.

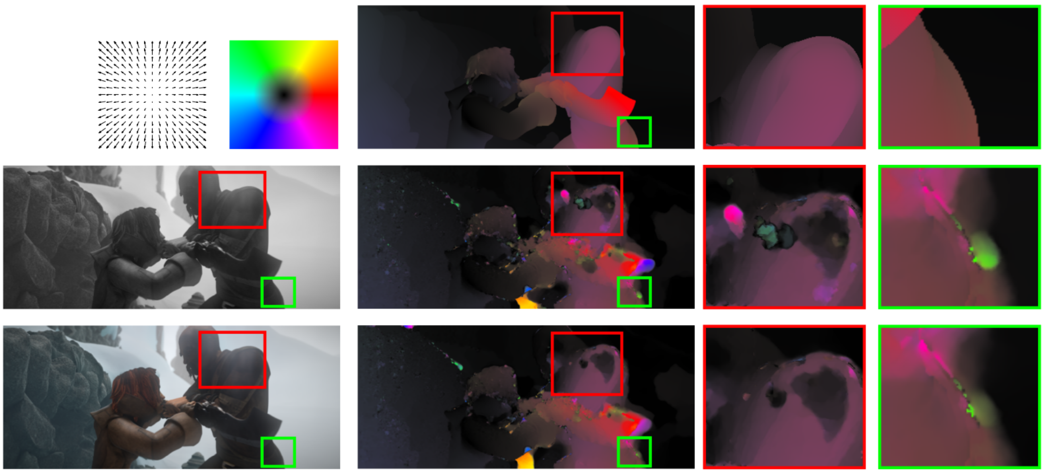

Figure 7: Motion details for Ambush 5.

[11] C. Fennema and W. Thompson. Velocity determination in scenes containing several moving objects. *Computer Graphics and Image Proccesings*, 9:301–315, 1979.

[12] Polina Golland and Alfred M. Bruckstein. Motion from color. *Computer Vision and Image Understanding*, 68(3):346–362, 1997.

[13] Berthold K. P. Horn and Brian G. Schunck. Determining optical flow. *Artificial Intelligence*, 17:185–203, 1981.

[14] Bruce D. Lucas and Takeo Kanade. An iterative image registration technique with an application to stereo vision. In *Proceedings of the 7th international joint conference on Artificial intelligence - Volume 2*, pages 674–679, San Francisco, CA, USA, 1981. Morgan Kaufmann Publishers Inc.

[15] V. Markandey and B.E. Flinchbaugh. Multispectral constraints for optical flow computation. In *Computer Vision, 1990. Proceedings, Third International Conference on*, pages 38–41, Dec 1990.

[16] Yana Mileva, Andrs Bruhn, and Joachim Weickert. Illumination-robust variational optical flow with photometric invariants. In FredA. Hamprecht, Christoph Schnrr, and Bernd Jhne, editors, *Pattern Recognition*, volume 4713 of *Lecture Notes in Computer Science*, pages 152–162. Springer Berlin Heidelberg, 2007.

[17] Nelson Monzón, Javier Sánchez, and Agustín Salgado. Optic flow: Improving discontinuity preserving. In *EUROCAST'13: Proceedings of the 14th international conference on Computer aided systems theory*, pages 114–116, Berlin, Heidelberg, 2013. Springer-Verlag.

[18] H H Nagel and W Enkelmann. An investigation of smoothness constraints for the estimation of displacement vector fields from image sequences. *IEEE Transanctions on Pattern Analysis and Machine Intelligence*, 8:565–593, September 1986.

[19] Naoya Ohta. Optical flow detection by color images. *IEEE International Conference on Image Processing*, pages 801–805, 1989.

[20] Agustín Salgado and Javier Sánchez. A temporal regularizer for large optical flow estimation. In *IEEE International Conference on Image Processing ICIP*, pages 1233–1236, 2006.

Table 2: AAE and EPE for the MPI Sintel dataset.

	AAE			**EPE**		
Sequence	**Grayscale**	**RGB**	%	**Grayscale**	**RGB**	%
Alley 1	3.343^o	3.328^o	**0.45**%	0.374	0.373	**0.27**%
Alley 2	3.100^o	3.065^o	**1.14**%	0.270	0.269	**0.37**%
Ambush 2	31.83^o	31.12^o	**2.28**%	25.14	25.22	**-0.32**%
Ambush 4	28.24^o	27.92^o	**1.14**%	34.73	34.72	**0.03**%
Ambush 5	29.59^o	26.91^o	**6.80**%	2.647	2.234	**18.5**%
Ambush 6	12.21^o	11.95^o	**2.17**%	12.72	12.62	**0.79**%
Ambush 7	6.924^o	6.821^o	**1.51**%	2.072	2.152	**-3.72**%
Bamboo 1	4.416^o	4.237^o	**4.22**%	0.307	0.291	**5.50**%
Bamboo 2	6.334^o	6.084^o	**4.10**%	0.706	0.665	**4.11**%
Bandage 1	7.367^o	7.262^o	**1.44**%	1.061	1.030	**3.01**%
Bandage 2	9.403^o	9.242^o	**1.74**%	1.145	1.074	**6.61**%
Cave 2	3.219^o	3.166^o	**1.67**%	1.707	1.741	**-1.95**%
Cave 4	13.19^o	12.60^o	**4.68**%	7.810	7.681	**1.68**%
Market 2	8.814^o	8.628^o	**2.15**%	1.561	1.607	**-2.86**%
Market 5	33.68^o	32.84^o	**2.55**%	27.37	25.08	**9.13**%
Market 6	6.491^o	6.070^o	**6.93**%	9.245	9.036	**2.31**%
Mountain 1	6.500^o	6.296^o	**3.24**%	1.407	1.273	**10.5**%
Shaman 2	6.367^o	6.335^o	**0.50**%	0.311	0.307	**1.30**%
Shaman 3	6.105^o	6.038^o	**1.11**%	0.508	0.520	**-2.31**%
Sleeping 1	1.394^o	1.290^o	**8.06**%	0.113	0.104	**8.65**%
Sleeping 2	1.589^o	1.541^o	**3.11**%	0.070	0.067	**4.47**%
Temple 2	7.579^o	7.296^o	**3.88**%	1.438	1.456	**-1.24**%
Temple 3	3.165^o	2.991^o	**5.82**%	0.958	0.886	**8.13**%

Table 3: Runtime for the Middlebury sequences (in seconds).

	Runtime		
Sequence	**Grayscale**	**RGB**	**Speed-up** (%)
Grove2	45	67	32.83%
Grove3	49	72	31.94%
Hydrangea	22	46	52.17%
RubberWhale	30	48	37.50%
Urban2	50	72	30.55%
Urban3	55	81	32.10%
Dimetrodon	28	47	40.42%

[21] Javier Sánchez, Agustín Salgado, and Nelson Monzón. Optical flow estimation with consistent spatio-temporal coherence models. In *International Conference on Computer Vision Theory and Applications (VISAPP)*, pages 366–370. Institute for Systems and Technologies of Information, Control and Communication, 2013.

[22] Steven A. Shafer. Using color to separate reflection components. *Color Research & Application*, 10(4):210–218, 1985.

[23] Javier Snchez Prez, Nelson Monzón Lpez, and Agustn Salgado de la Nuez. Robust Optical Flow Estimation. *Image Processing On Line*, 2013:252–270, 2013.

[24] J. van de Weijer and T. Gevers. Robust optical flow from photometric invariants. In *Image Processing, 2004. ICIP '04. 2004 International Conference on*, volume 3, pages

Table 4: Runtime for the MPI Sintel dataset (in seconds).

	Runtime		
Sequence	**Grayscale**	**RGB**	**Speed-up** (%)
Alley 1	63	107	41.12%
Alley 2	49	81	39.51%
Ambush 2	199	150	-32.67%
Ambush 4	70	106	33.96%
Ambush 5	102	135	24.45%
Ambush 6	99	140	29.29%
Ambush 7	97	144	32.64%
Bamboo 1	64	116	44.83%
Bamboo 2	79	108	26.85%
Bandage 1	89	128	30.47%
Bandage 2	93	128	27.34%
Cave 2	84	113	25.66%
Cave 4	86	120	28.33%
Market 2	73	114	35.96%
Market 5	205	205	0.00%
Market 6	104	136	23.53%
Mountain 1	45	81	44.45%
Shaman 2	67	101	33.66%
Shaman 3	89	123	27.64%
Sleeping 1	31	63	50.79%
Sleeping 2	36	68	47.06%
Temple 2	92	131	29.77%
Temple 3	90	124	27.42%

1835–1838 Vol. 3, Oct 2004.

[25] Andreas Wedel, Daniel Cremers, Thomas Pock, and Horst Bischof. Structure- and motion-adaptive regularization for high accuracy optic flow. In *IEEE International Conference on Computer Vision*, pages 1663–1668, September 2009.

[26] Joachim Weickert and Christoph Schnörr. Variational Optic Flow Computation with a Spatio-Temporal Smoothness Constraint. *Journal of Mathematical Imaging and Vision*, 14(3):245–255, May 2001.

[27] Li Xu, Jiaya Jia, and Yasuyuki Matsushita. Motion detail preserving optical flow estimation. In *IEEE Conference on Computer Vision and Pattern Recognition (CVPR)*, pages 1293–1300, June 2010.

[28] Henning Zimmer, Andrs Bruhn, and Joachim Weickert. Optic flow in harmony. *International Journal of Computer Vision*, 93(3):368–388, 2011.

Centro de Tecnologías de la Imagen
Universidad de Las Palmas de Gran Canaria
http://www.ctim.es